crystals

MDPI

Article

Polarized Light Microscopy Study on the Reentrant Phase Transition in a $(Ba_{1-x}K_x)Fe_2As_2$ Single Crystal with $x = 0.24$

Yong Liu [1,*], Makariy A. Tanatar [1,2], Erik Timmons [1,2] and Thomas A. Lograsso [1,3]

1 Division of Materials Sciences and Engineering, Ames Laboratory, U.S. Department of Energy, Ames, IA 50011, USA; tanatar@iastate.edu (M.A.T.); erikt@iastate.edu (E.T.); lograsso@ameslab.gov (T.A.L.)
2 Department of Physics and Astronomy, Iowa State University, Ames, IA 50011, USA
3 Department of Materials Science and Engineering, Iowa State University, Ames, IA 50011, USA
* Correspondence: yliu@ameslab.gov; Tel.: +1-515-294-2975; Fax: +1-515-294-8727

Academic Editor: Haidong Zhou
Received: 1 September 2016; Accepted: 4 November 2016; Published: 9 November 2016

Abstract: A sequence of structural/magnetic transitions on cooling is reported in the literature for hole-doped iron-based superconductor $(Ba_{1-x}K_x)Fe_2As_2$ with $x = 0.24$. By using polarized light microscopy, we directly observe the formation of orthorhombic domains in $(Ba_{1-x}K_x)Fe_2As_2$ ($x = 0.24$) single crystal below a temperature of simultaneous structural/magnetic transition T_N ~80 K. The structural domains vanish below ~30 K, but reappear below $T = 15$ K. Our results are consistent with reentrance transformation sequence from high-temperature tetragonal (HTT) to low temperature orthorhombic (LTO1) structure at T_N ~80 K, LTO1 to low temperature tetragonal (LTT) structure at T_c ~25 K, and LTT to low temperature orthorhombic (LTO2) structure at T ~15 K.

Keywords: reentrant phase transition; polarized optical images; structural domains

1. Introduction

Iron-based superconductors show rich composition and pressure dependences of phase diagrams [1–3]. Similar to high T_c cuprates—heavy fermion and organic superconductors [4]—the dome of superconductivity emerges on suppression of magnetic order, with maximum T_c in the vicinity of a putative quantum critical point where magnetism vanishes. Contrary to the cuprates—in which magnetic order is of Neel type [5]—the parent compounds of iron-based compounds *Ln*OFeAs (*Ln* = rare earth metals) and $AeFe_2As_2$ (*Ae* = alkaline earth metals) show a magnetic transition into stripy antiferromagnetic phase [1], preceded or concomitant with a phase transition from high-temperature tetragonal (HTT, referred to C_4 phase) to low-temperature orthorhombic (LTO, referred to C_2 phase) structure. Even more complicated phase diagrams are reported for hole-doped $(Ba_{1-x}K_x)Fe_2As_2$, both under pressure [6,7] and at ambient pressure [8]. Similar anomaly in a much broader composition range is observed in $(Ba_{1-x}Na_x)Fe_2As_2$ [9,10] and $(Sr_{1-x}Na_x)Fe_2As_2$ [11]. The anomaly was linked to a phase reentrant behavior from low-temperature orthorhombic (LTO C_2 phase) to low-temperature tetragonal (LTT C_4 phase) structure [8–11].

In $(Ba_{1-x}K_x)Fe_2As_2$, the anomaly was overlooked in early studies on polycrystalline material [12] and in single crystals [13,14], since it is found only in a very narrow doping range ($0.24 < x < 0.27$) in the phase diagrams, on the verge of magnetism suppression. Spanning Δx ~0.14 in composition, the LTT C_4 phase in $(Sr_{1-x}Na_x)Fe_2As_2$ is found to extend over a larger range of compositions, and to exhibit a significantly higher transition temperature, T_{re} ~65 K, than in either of the other systems in which it has been observed [11]. Interestingly, the magnetic moments in the high temperature C_2 phase are aligned in the *ab* plane, but they reorient on cooling below T_{re}, and point along the *c* direction in $(Ba_{1-x}Na_x)Fe_2As_2$ with $x = 0.35$ [15].

In previous studies, the tetragonal-to-orthorhombic reentrant transition was revealed by neutron and X-ray diffraction measurements [9,11] and high-resolution thermal-expansion and specific-heat measurements [8,10]. It should be pointed out that the orthorhombic distortion leads to the formation of structural domains in the LTO state, revealed and quantified by using polarized light microscopy [16–20]. Here, we use polarized light microscopy to study the temperature evolution of orthorhombic domain patterns in a single crystal of $(Ba_{1-x}K_x)Fe_2As_2$ (x = 0.24). The observed appearance, disappearance, and reappearance of domain patterns on cooling are consistent with previous reports of the transformation sequence.

2. Results and Discussion

Although large single crystals are easily obtained by self-flux method, we find that the composition of the crystals varies significantly over the boule, as reflected in the measured characteristic transition temperatures. Superconducting transition temperatures T_cs of cleaved small plates span nearly 8 K from the top to the bottom of a large bulk crystal. Furthermore, some of cleaved crystals show a broad transition, due to the distribution of x. For our further study, we selected only samples showing sharp superconducting transitions in magnetization measurements, as illustrated in Figure 1a. Figure 1b shows the temperature dependence of resistivity of $(Ba_{1-x}K_x)Fe_2As_2$ (x = 0.24). The superconducting transition temperatures as determined by two measurements match quite well. The temperature-dependent resistivity derivative—dρ/dT vs. T (inset in Figure 1b)—shows a clear dip at T_N = 80.8 K, which signals the simultaneous orthorhombic/antiferromagnetic transition. These values of $T_c(x = 0.24)$ = 26 K and $T_N(x = 0.24)$ = 80.8 K match very well with literature values $T_c(x = 0.24)$ = 26 K and $T_N(x = 0.24)$ = 79 K [21], showing correct x determination.

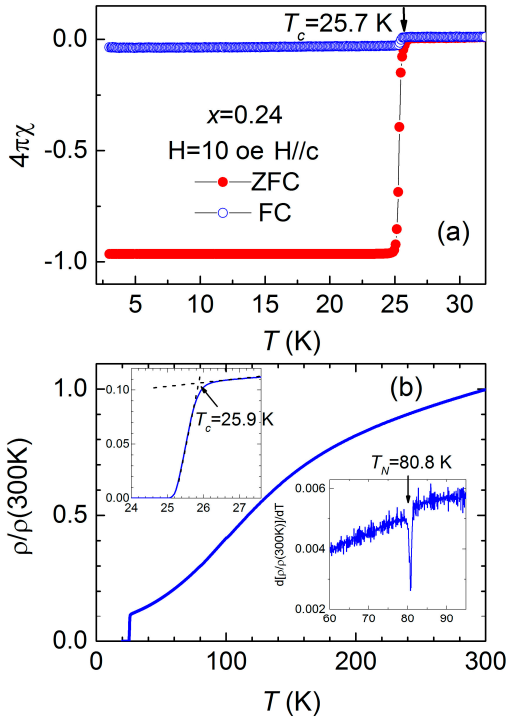

Figure 1. (**a**) Temperature dependence of magnetization for the $(Ba_{1-x}K_x)Fe_2As_2$ single crystal (x = 0.24) used in resistivity and polarized optics studies. The sample was cooled in zero magnetic field from above T_c to 3 K (ZFC) and with an applied field of 10 Oe (FC). The data were collected during the warming of the sample from 3 K to 35 K; (**b**) Normalized temperature-dependent resistivity of a sample, cut from part of magnetization crystal after polarized optics study. The derivate of the normalized resistivity (inset in panel b) shows a clear dip as the sample undergoes structure and magnetic transition at T_N = 80.8 K.

Figure 2 shows the temperature dependence of polarized light images of the cleaved surface of $(Ba_{1-x}K_x)Fe_2As_2$ (x = 0.24) single crystal, used in magnetization measurements (Figure 1a). The cleavage plane is a tetragonal (001) plane. The image of the sample at 80 K reveals a regular pattern of domain boundaries running in two orthogonal directions (close to horizontal and vertical directions) as shown by the dashed lines. These lines show temperature evolution, and should be distinguished from temperature-independent features observed in the bottom left corners of the image patterns, representing terraces on the sample surface. The domain wall pattern represents boundaries of 45° domains [16] and runs parallel to tetragonal (100) and (010) directions. The temperature of the domain pattern formation is consistent with the temperature of the simultaneous structural/magnetic transition, as determined from a position of a dip in the temperature-dependent resistivity derivative (inset in Figure 1b), positioned at T_N = 80.8 K. The domain formation below T_N is observed in parent [16] and both electron [17] and hole [18] doped $AeFe_2As_2$. This is due to random orientation of the directions of orthorhombic a_O and b_O axes of the orthorhombic phase, rotated by 45° from the a_T axis in the tetragonal lattice symmetry. There is a slight volume change in the unit cell before and after the structural phase transition at T_N [22]. The orthorhombic distortion defined as $\delta = (a_O - b_O) / (a_O + b_O)$ increases from zero to 2×10^{-3} on cooling [22]. The tensile stresses accompanying the transformation are partially released by the formation of domain twin boundaries (lines in Figure 2), leading to the formation of 45°-type structural domains, with walls running parallel to the [001] direction of the lattice [16].

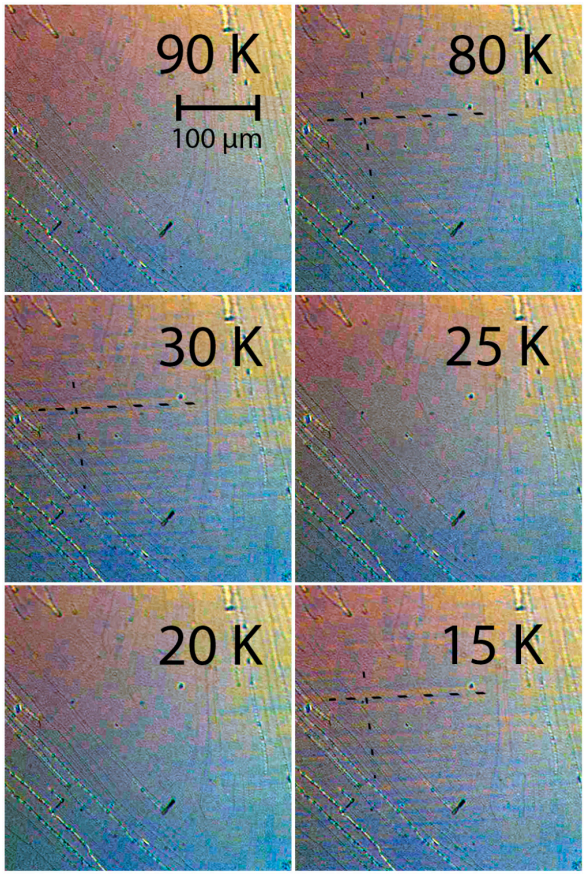

Figure 2. Temperature evolution of polarized optical images of the $(Ba_{1-x}K_x)Fe_2As_2$ (x = 0.24) single crystal. Scale bar corresponds to 100 μm. The sequence shows the appearance of orthorhombic/magnetic domains at 80 K, highlighted with dashed lines to guide the eyes (horizontal lines in the center of the image panels). The domains are clearly visible on cooling down to 30 K, but disappear at 25 K. They reappear at 15 K. The scratch-like lines running at approximately 45° inclination in the left-bottom corner of the image panels correspond to growth terraces and faults.

The domain pattern in $(Ba_{1-x}K_x)Fe_2As_2$ (x = 0.24) remains stable down to 30 K. With further cooling down to T = 25 K, the domains vanish, which is contrary to observations in parent and lower-doped $(Ba_{1-x}K_x)Fe_2As_2$ samples [16,18]. Interestingly, the domain pattern emerges again at T = 15 K. This sequence of transformations is consistent with reentrant transformation into tetragonal phase [8].

In Figure 3, we compare the observations of our study with the doping dependence of the phase diagram of $(Ba_{1-x}K_x)Fe_2As_2$ as determined from thermal expansion and heat capacity measurements [8]. Due to possible error in composition determination with different techniques, it is more appropriate to compare sample transition temperatures, rather than composition x. The T_N of our sample (80.8 K) is somewhat higher than that in samples at the center of the anomaly [8], suggesting that our sample is located to the left (lower x) in the doping phase diagram. The domain disappearance/reappearance features in the polarized optical images (Figure 2) are found at temperatures which are in reasonable agreement with T_{re1} and T_{re2} features.

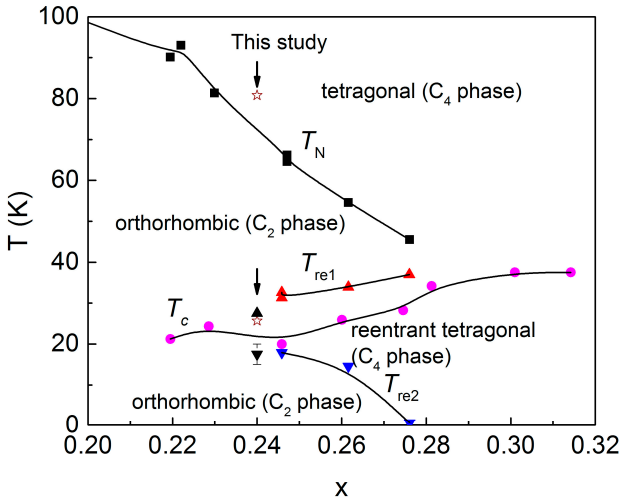

Figure 3. Composition–temperature phase diagram of reentrant C_2-C_4-C_2 transformation in $(Ba_{1-x}K_x)Fe_2As_2$ (after Refs. [7,8]). The data of this study are shown with stars and highlighted by arrows. They are in reasonable agreement with the diagram, within possible error bars of composition determination.

In the iron-based superconductors, the iron spins order antiferromagnetically in a stripe pattern below T_N with a wavevector of either **Q**1 = (π,0) or **Q**2 = (0,π). The formation of magnetic stripe structure is accompanied by the C_4 (HTT phase)-C_2 (LTO phase) phase via magnetoelastic coupling at T_N [1,2]. In the hole-doped $(Sr_{1-x}Na_x)Fe_2As_2$, Mössbauer data revealed that the reentrant C_4 phase is characteristic of a double-**Q** magnetic structure below T_{re}, where magnetic structure comprises the superposition of two orthogonal stripes (i.e., **Q**1 and **Q**2) [23]. It should be pointed out that the C_2 phase could be restored in $(Ba_{1-x}Ka_x)Fe_2As_2$ below T_{re2} (see Figure 3). However, the reentrant C_4 phase is robust in $(Ba_{1-x}Na_x)Fe_2As_2$ [9,10] and $(Sr_{1-x}Na_x)Fe_2As_2$ [11] when cooled down to low temperatures. Here, the disorder and strain caused by the large mismatch of ionic radius of dopants may stabilize double-Q order (i.e., C_4 phase) [24]. The fact that the interplay between magnetic and lattice structures leads to reentrant phase transition is manifested in other compounds. For example, $BaFe_2(PO4)_2$ undergoes a rare reentrant structural transition owing to the competition between uniaxial magnetism and the Jahn–Teller distortion [25,26].

3. Materials and Methods

Single crystals of $(Ba_{1-x}K_x)Fe_2As_2$ were grown by using the self-flux method. Details of the synthesis and characterization can be found elsewhere [27,28]. Briefly, the starting materials of

Ba and K lump, and Fe and As powder were weighed and loaded into an alumina crucible in a glovebox. The alumina crucible was sealed in a tantalum tube by arc welding. The tantalum tube was sealed in a quartz ampoule to prevent the tantalum tube from oxidizing in the furnace. We developed an inverted-temperature-gradient method [28] to grow large and high-quality single crystals of $(Ba_{1-x}K_x)Fe_2As_2$. The crystallization processes from the top of a liquid melt helps to expel impurity phases during crystal growth, as shown in Figure 4.

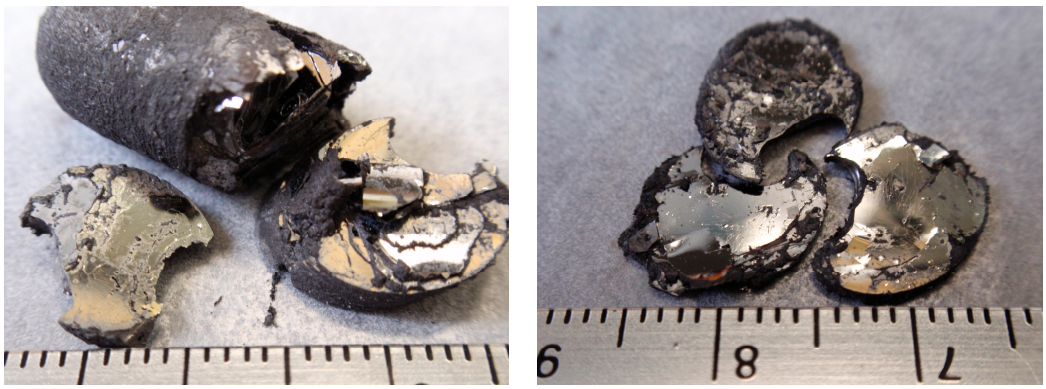

(**a**) (**b**)

Figure 4. (**a**) Photos of $(Ba_{1-x}K_x)Fe_2As_2$ single crystals grown by a self-flux method; (**b**) The disk-like crystals (~1 mm in thickness and 10 mm in diameter) are formed in the top of the ingot.

The composition of the crystals was determined using wavelength dispersion X-ray spectroscopy (WDS) (JEOL 8200 Electron Microprobe, JEOL, Peabody, MA, USA) of electron microprobe analysis. The polarized optical images were taken in a Leica DMLM microscope (Leica Microsystems Wetzlar GmbH, Wetzlar, Germany) with polarizer and analyzer. A helium flow cryostat was positioned on the x–y–z stage of the microscope and allowed direct imaging from room temperature down to 5 K.

Magnetization was measured by using Physical Property Measurement System (PPMS) equipped with Vibrating Sample Magnetometer (VSM) (Quantum Design, San Diego, CA, USA), and in-plane resistivity ϱ_{ab} was measured using the AC transport option of PPMS.

White-light optical images were taken in a Leica Digital & Light Microscope (DMLM) polarization microscope with polarizer and analyzer in almost crossed position. They were taken in reflection mode on cleaved sample (001) plane. A helium flow cryostat was positioned on the x–y stage of the microscope and allowed direct imaging from room temperature down to 5 K. High resolution static images video were recorded. The contrast of the domain images is higher for larger difference in the rotation of the polarization plane between neighboring domains, proportional to the degree of orthorhombic distortion, $\delta = (a_O - b_O) / (a_O + b_O)$. Quantitative analysis of the images enables in determination of the orthorhombic order parameter [19,20]. This was not possible due to low contrast of the images.

4. Conclusions

Large single crystals of $(Ba_{1-x}K_x)Fe_2As_2$ were grown by self-flux method. Magnetization measurements were used to screen large pieces of $(Ba_{1-x}K_x)Fe_2As_2$ single crystals, with homogeneous samples selected using superconducting transition width as a criterion. Samples with T_c of 25 K were used to study tetragonal-orthorhombic-tetragonal-orthorhombic transformation sequence using resistivity and polarized optical imaging. We found domain formation at T_N = 80 K, as common for underdoped iron-based superconductors. Contrary to all previous cases, though, the pattern shows transformation with cooling. Our observations are in agreement with reentrant orthorhombic transformation in the material.

Acknowledgments: We thank Warren E. Straszheim for WDS measurement and Ruslan Prozorov for support of this study. This work was supported by the U.S. Department of Energy (DOE), Office of Basic Energy Sciences, Materials Science and Engineering Division. Ames Laboratory is operated for the U.S. DOE by Iowa State University under Contract No. DE-AC02-07CH11358.

Author Contributions: Yong Liu and Makariy A. Tanatar conceived and designed the experiments; Yong Liu and Thomas A. Lograsso grew the single crystals; Yong Liu performed magnetization measurement, Makariy A. Tanatar performed resistivity measurement, Makariy A. Tanatar and Erik Timmons performed polarized optical microscopy measurement, Yong Liu and Makariy A. Tanatar analyzed the data and wrote the paper, Thomas A. Lograsso supervised project.

Conflicts of Interest: The authors declare no conflict of interest.

References

1. Johnston, D.C. The puzzle of high temperature superconductivity in layered iron pnictides and chalcogenides. *Adv. Phys.* **2010**, *59*, 803–1061. [CrossRef]
2. Stewart, G.R. Superconductivity in iron compounds. *Rev. Mod. Phys.* **2011**, *83*, 1589. [CrossRef]
3. Canfield, P.C.; Bud'ko, S.L. FeAs-Based Superconductivity: A Case Study of the Effects of Transition Metal Doping on $BaFe_2As_2$. *Annu. Rev. Condens. Matter Phys.* **2010**, *1*, 27. [CrossRef]
4. Taillefer, L. Scattering and Pairing in Cuprate Superconductors. *Annu. Rev. Condens. Matter Phys.* **2010**, *1*, 51. [CrossRef]
5. Vaknin, D.; Sinha, S.K.; Moncton, D.E.; Johnston, D.C.; Newsam, J.M.; Safinya, C.R.; King, H.E., Jr. Antiferromagnetism in La_2CuO_{4-y}. *Phys. Rev. Lett.* **1987**, *58*, 2802. [CrossRef] [PubMed]
6. Hassinger, E.; Gredat, G.; Valade, F.; René de Cotret, S.; Juneau-Fecteau, A.; Reid, J.-Ph.; Kim, H.; Tanatar, M.A.; Prozorov, R.; Shen, B.; et al. Pressure-induced Fermi-surface reconstruction in the iron-arsenide superconductor $Ba_{1-x}K_xFe_2As_2$: Evidence of a phase transition inside the antiferromagnetic phase. *Phys. Rev. B* **2012**, *86*, 140502(R). [CrossRef]
7. Hassinger, E.; Gredat, G.; Valade, F.; René de Cotret, S.; Cyr-Choinière, O.; Juneau-Fecteau, A.; Reid, J.-Ph.; Kim, H.; Tanatar, M.A.; Prozorov, R.; et al. Expansion of the tetragonal magnetic phase with pressure in the iron arsenide superconductor $Ba_{1-x}K_xFe_2As_2$. *Phys. Rev. B* **2016**, *93*, 144401. [CrossRef]
8. Böhmer, A.E.; Hardy, F.; Wang, L.; Wolf, T.; Schweiss, P.; Meingast, C. Superconductivity-induced re-entrance of the orthorhombic distortion in $Ba_{1-x}K_xFe_2As_2$. *Nat. Commun.* **2015**, *6*, 7911. [CrossRef] [PubMed]
9. Avci, S.; Chmaissem, O.; Allred, J.M.; Rosenkranz, S.; Eremin, I.; Chubukov, A.V.; Bugaris, D.E.; Chung, D.Y.; Kanatzidis, M.G.; Castellan, J.-P.; et al. Magnetically driven suppression of nematic order in an iron-based superconductor. *Nat. Commun.* **2014**, *5*, 3845. [CrossRef] [PubMed]
10. Wang, L.; Hardy, F.; Böhmer, A.E.; Wolf, T.; Schweiss, P.; Meingast, C. Complex phase diagram of $Ba_{1-x}Na_xFe_2As_2$: A multitude of phases striving for the electronic entropy. *Phys. Rev. B* **2016**, *93*, 014514. [CrossRef]
11. Taddei, K.M.; Allred, J.M.; Bugaris, D.E.; Lapidus, S.; Krogstad, M.J.; Stadel, R.; Claus, H.; Chung, D.Y.; Kanatzidis, M.G.; Rosenkranz, S.; et al. Detailed magnetic and structural analysis mapping a robust magnetic C4 dome in $Sr_{1-x}Na_xFe_2As_2$. *Phys. Rev. B* **2016**, *93*, 134510. [CrossRef]
12. Rotter, M.; Pangerl, M.; Tegel, M.; Johrendt, D. Superconductivity and Crystal Structures of $(Ba_{1-x}K_x)Fe_2As_2$ ($x = 0 - 1$). *Angew. Chem. Int. Ed.* **2008**, *47*, 7949–7952. [CrossRef] [PubMed]
13. Luo, H.Q.; Wang, Z.S.; Yang, H.; Cheng, P.; Zhu, X.; Wen, H.-H. Growth and characterization of $A_{1-x}K_xFe_2As_2$ (A = Ba, Sr) single crystals with $x = 0 - 0.4$. *Supercond. Sci. Technol.* **2008**, *21*, 125014. [CrossRef]
14. Tanatar, M.A.; Straszheim, W.E.; Kim, H.; Murphy, J.; Spyrison, N.; Blomberg, E.C.; Cho, K.; Reid, J.-Ph.; Shen, B.; Taillefer, L.; et al. Interplane resistivity of underdoped single crystals $(Ba_{1-x}K_x)Fe_2As_2$ ($0 \leq x < 0.34$). *Phys. Rev. B* **2014**, *89*, 144514.
15. Waßer, F.; Schneidewind, A.; Sidis, Y.; Wurmehl, S.; Aswartham, S.; Büchner, B.; Braden, M. Spin reorientation in $Ba_{0.65}Na_{0.35}Fe_2As_2$ studied by single-crystal neutron diffraction. *Phys. Rev. B* **2015**, *91*, 060505(R). [CrossRef]
16. Tanatar, M.A.; Kreyssig, A.; Nandi, S.; Ni, N.; Bud'ko, S.L.; Canfield, P.C.; Goldman, A.I.; Prozorov, R. Direct imaging of the structural domains in the iron pnictides AFe_2As_2 (A = Ca,Sr,Ba). *Phys. Rev. B* **2009**, *79*, 180508(R). [CrossRef]

17. Prozorov, R.; Tanatar, M.A.; Ni, N.; Kreyssig, A.; Nandi, S.; Bud'ko, S.L.; Goldman, A.I.; Canfield, P.C. Intrinsic pinning on structural domains in underdoped single crystals of $Ba(Fe_{1-x}Co_x)_2As_2$. *Phys. Rev. B* **2009**, *80*, 174517. [CrossRef]
18. Blomberg, E.C.; Tanatar, M.A.; Fernandes, R.M.; Mazin, I.I.; Shen, B.; Wen, H.-H.; Johannes, M.D.; Schmalian, J.; Prozorov, R. Sign-reversal of the in-plane resistivity anisotropy in hole-doped iron pnictides. *Nat. Commun.* **2013**, *4*, 1914. [CrossRef] [PubMed]
19. Blomberg, E.C.; Kreyssig, A.; Tanatar, M.A.; Fernandes, R.M.; Kim, M.G.; Thaler, A.; Schmalian, J.; Bud'ko, S.L.; Canfield, P.C.; Goldman, A.I.; et al. Effect of tensile stress on the in-plane resistivity anisotropy in $BaFe_2As_2$. *Phys. Rev. B* **2012**, *85*, 144509. [CrossRef]
20. Tanatar, M.A.; Böhmer, A.E.; Timmons, E.I.; Schütt, M.; Drachuck, G.; Taufour, V.; Kothapalli, K.; Kreyssig, A.; Bud'ko, S.L.; Canfield, P.C.; et al. Origin of the Resistivity Anisotropy in the Nematic Phase of FeSe. *Phys. Rev. Lett.* **2016**, *117*, 127001. [CrossRef] [PubMed]
21. Avci, S.; Chmaissem, O.; Chung, D.Y.; Rosenkranz, S.; Goremychkin, E.A.; Castellan, J.P.; Todorov, I.S.; Schlueter, J.A.; Claus, H.; Daoud-Aladine, A.; et al. Phase diagram of $Ba_{1-x}K_xFe_2As_2$. *Phys. Rev. B* **2012**, *85*, 184507. [CrossRef]
22. Allred, J.M.; Avci, S.; Chung, D.Y.; Claus, H.; Khalyavin, D.D.; Manuel, P.; Taddei, K.M.; Kanatzidis, M.G.; Rosenkranz, S.; Osborn, R.; et al. Tetragonal magnetic phase in $Ba_{1-x}K_xFe_2As_2$ from X-ray and neutron diffraction. *Phys. Rev. B* **2015**, *92*, 094515. [CrossRef]
23. Allred, J.M.; Taddei, K.M.; Bugaris, D.E.; Krogstad, M.J.; Lapidus, S.H.; Chung, D.Y.; Claus, H.; Kanatzidis, M.G.; Brown, D.E.; Kang, J.; et al. Double-Q spin-density wave in iron arsenide superconductors. *Nat. Phys.* **2016**, *12*, 493. [CrossRef]
24. Gastiasoro, M.N.; Andersen, B.M. Competing magnetic double-Q phases and superconductivity-induced reentrance of C_2 magnetic stripe order in iron pnictides. *Phys. Rev. B* **2015**, *92*, 140506(R). [CrossRef]
25. David, R.; Pautrat, A.; Filimonov, D.; Kabbour, H.; Vezin, H.; Whangbo, M.-H.; Mentré, O. Across the structural re-entrant transition in $BaFe_2(PO_4)_2$: Influence of the two-dimensional ferromagnetism. *J. Am. Chem. Soc.* **2013**, *135*, 13023–13029. [CrossRef] [PubMed]
26. Kabbour, H.; David, R.; Pautrat, A.; Koo, H.-J.; Whangbo, M.-H.; André, G.; Mentré, O. A genuine two-dimensional Ising ferromagnet with magnetically driven re-entrant transition. *Angew. Chem. Int. Ed.* **2012**, *51*, 11745–11749. [CrossRef] [PubMed]
27. Liu, Y.; Tanatar, M.A.; Kogan, V.G.; Kim, H.; Lograsso, T.A.; Prozorov, R. Upper critical field of high-quality single crystals of KFe_2As_2. *Phys. Rev. B* **2013**, *87*, 134513. [CrossRef]
28. Liu, Y.; Tanatar, M.A.; Straszheim, W.E.; Jensen, B.; Dennis, K.W.; McCallum, R.W.; Kogan, V.G.; Prozorov, R.; Lograsso, T.A. Comprehensive scenario for single-crystal growth and doping dependence of resistivity and anisotropic upper critical fields in $(Ba_{1-x}K_x)Fe_2As_2$ ($0.22 \leq x \leq 1$). *Phys. Rev. B* **2014**, *89*, 134504. [CrossRef]